

LA-UR-

97-3481

Approved for public release;
distribution is unlimited.

CONF-9707100--

Title:

RADIOGRAPHIC LEAST-SQUARE FITTING
TECHNIQUE ACCURATELY MEASURES
DIMENSIONS AND X-RAY ATTENUATION

Author(s):

Thomas A. Kelley, CIC-12
David M. Stupin, ESA-MT

RECEIVED

OCT 01 1997

OSTI

Submitted to:

Review of Progress in Quantitative
Nondestructive Evaluation, Vol. 17.
Edited by D.O. Thompson and D.E.
Chimenti, Plenum Publishing
Corporation, New York, NY 10013.
(Proceedings of the Twenty-Fourth
Annual Review of Progress in
Quantitative Nondestructive Evaluation,
San Diego, CA, July 27-August 1, 1997.)

MASTER

DISTRIBUTION OF THIS DOCUMENT IS UNLIMITED

Los Alamos
NATIONAL LABORATORY

Los Alamos National Laboratory, an affirmative action/equal opportunity employer, is operated by the University of California for the U.S. Department of Energy under contract W-7405-ENG-36. By acceptance of this article, the publisher recognizes that the U.S. Government retains a nonexclusive, royalty-free license to publish or reproduce the published form of this contribution, or to allow others to do so, for U.S. Government purposes. Los Alamos National Laboratory requests that the publisher identify this article as work performed under the auspices of the U.S. Department of Energy. The Los Alamos National Laboratory strongly supports academic freedom and a researcher's right to publish; as an institution, however, the Laboratory does not endorse the viewpoint of a publication or guarantee its technical correctness.

DISCLAIMER

This report was prepared as an account of work sponsored by an agency of the United States Government. Neither the United States Government nor any agency thereof, nor any of their employees, make any warranty, express or implied, or assumes any legal liability or responsibility for the accuracy, completeness, or usefulness of any information, apparatus, product, or process disclosed, or represents that its use would not infringe privately owned rights. Reference herein to any specific commercial product, process, or service by trade name, trademark, manufacturer, or otherwise does not necessarily constitute or imply its endorsement, recommendation, or favoring by the United States Government or any agency thereof. The views and opinions of authors expressed herein do not necessarily state or reflect those of the United States Government or any agency thereof.

DISCLAIMER

**Portions of this document may be illegible
in electronic image products. Images are
produced from the best available original
document.**

RADIOGRAPHIC LEAST SQUARES FITTING TECHNIQUE ACCURATELY MEASURES DIMENSIONS AND X-RAY ATTENUATION

Thomas A. Kelley
CIC-12
Los Alamos National Laboratory
Los Alamos, NM 87545

David M. Stupin
ESA-MT
Los Alamos National Laboratory
Los Alamos, NM 87545

INTRODUCTION

In support of stockpile stewardship and other important nondestructive test (NDT) applications, we seek improved methods for rapid evaluation of materials to detect degradation, warping, and shrinkage. Typically, such tests involve manual measurements of dimensions on radiographs. We seek to speed the process and reduce the costs of performing NDT by analyzing radiographic data using a least-square fitting technique for rapid evaluation of industrial parts. In 1985, Whitman, Hanson, and Mueller have demonstrated a least-square fitting technique that very accurately locates the edges of cylindrically symmetrical objects in radiographs. [1] To test the feasibility of applying this technique to a large number of parts, we examine whether an automated least squares algorithm can be routinely used for measuring the dimensions and attenuations of materials in two nested cylinders. The proposed technique involves making digital radiographs of the cylinders and analyzing the images. In our preliminary study, however, we use computer simulations of radiographs.

MODEL USED

In our study, we simulated radiographs of two nested, concentric cylinders where the outer cylinder was thicker than the inner cylinder by a factor of ten. We assume that the material in each cylinder is homogeneous. Attenuation of x-rays in each cylinder is measured by an attenuation parameter, the product of the attenuation coefficient μ of the material and the density ρ of that material. The inner cylinder is much denser than the outer cylinder and should exhibit more x-ray attenuation. For the purpose of constructing a model, we assume that the thickness of the outer cylinder is ten times greater than that of the inner cylinder. We also assume that the attenuation parameter for the inner cylinder is 3.5 times larger than that for the outer cylinder.

Finally, building on the assumption that the x-rays penetrate the object in a direction perpendicular to the axis of the cylinders, we can construct a plot of the ideal transmission through these cylinders. Figure 1 represents the ideal relative transmission through the two cylinders, assuming a point source for the x-rays, no blurring of the x-rays, and no noise.

The vertical scale measures the relative intensity of the x-rays that reach the detector. The horizontal scale is the relative position, in pixels, from one side of the digitized radiographic image. Looking at this plot from left to right, the first dip in the transmission is due to the attenuation of the x-rays through the outer cylinder. The second dip is due to the added attenuation in passing through the inner cylinder. The central portion of the plot corresponds to the passage through both cylinders and the empty interior of the two cylinders. The rise in the middle is due to a decrease in the x-ray path length.

The mathematical function used to generate this plot is given as:

$$Y_i = \exp\left(\sum_{n=1}^2 b_n P_n(X_i)\right) \quad (1)$$

where the attenuation parameter in the n th cylinder is given by $b_n = -\mu_n \rho_n$ and the path length through the n th cylinder, $P_n(X)$ is given by

$$P_n(X) = 2F_n(X)\sqrt{S_n^2 - (X-C)^2} - 2G_n(X)\sqrt{R_n^2 - (X-C)^2}. \quad (2)$$

μ_n is the x-ray attenuation coefficient of the n th shell and ρ_n is the density of the material in the n th shell. The sum in the formula for Y is taken over the two cylinders in the object.

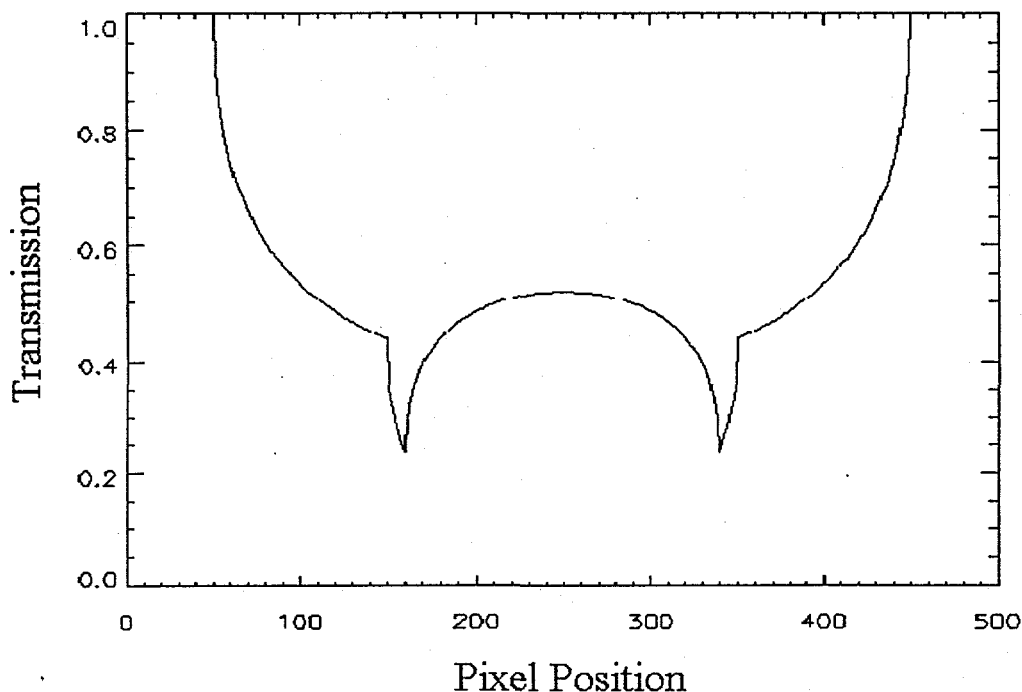


Figure 1. Plot of ideal relative transmission through a set of two nested cylinders as a function of position in pixels.

S_n , R_n , and C , refer respectively to the outer radius of the n th cylinder, the inner radius of the n th cylinder and the common center position of the two cylinders. Note that all these dimensions are in pixels. $F_n(X)$ and $G_n(X)$ are indicator functions. $F_n(X)$ is 1 when $(|X-C| < S_n)$ and 0 otherwise. $G_n(X)$ is 1 when $(|X-C| < R_n)$ and 0 otherwise.

Figure 2 illustrates how we arrive at the above formulas for path length $P(X)$. In particular, it shows one half of the cross section of an arbitrary cylinder with center at position C , an inner radius of R , and an outer radius of S . We assume that the x-rays are directed from above and penetrate the cylinder at position X . The vertical line in the left portion of the figure shows a path that does not pass through the interior of the cylinder. The length of the line is given by

$$\sqrt{S^2 - (X - C)^2}. \quad (3)$$

The vertical line in the right portion of the figure shows a path that does pass through the interior of the cylinder. The length of the path in the shaded portion is given by

$$\sqrt{S^2 - (X - C)^2} - \sqrt{R^2 - (X - C)^2}. \quad (4)$$

Given a realistic set of transmission data which includes blurring and noise, our goal is to determine the values of the 7 parameters b_1 , b_2 , S_1 , S_2 , R_1 , R_2 , and C which generate a curve that best fits the actual data. This is a non-linear problem requiring an iterative algorithm. It is challenging to find non-linear least squares algorithms that converge at all, much less converge to the global minimum. These algorithms generally rely on the gradient vector in parameter space. For this problem, the gradient vector as a function of pixel position has discontinuities that hamper the search algorithm. Because of this, it is important to produce a good set of initial estimates for the parameters before starting any least squares algorithm.

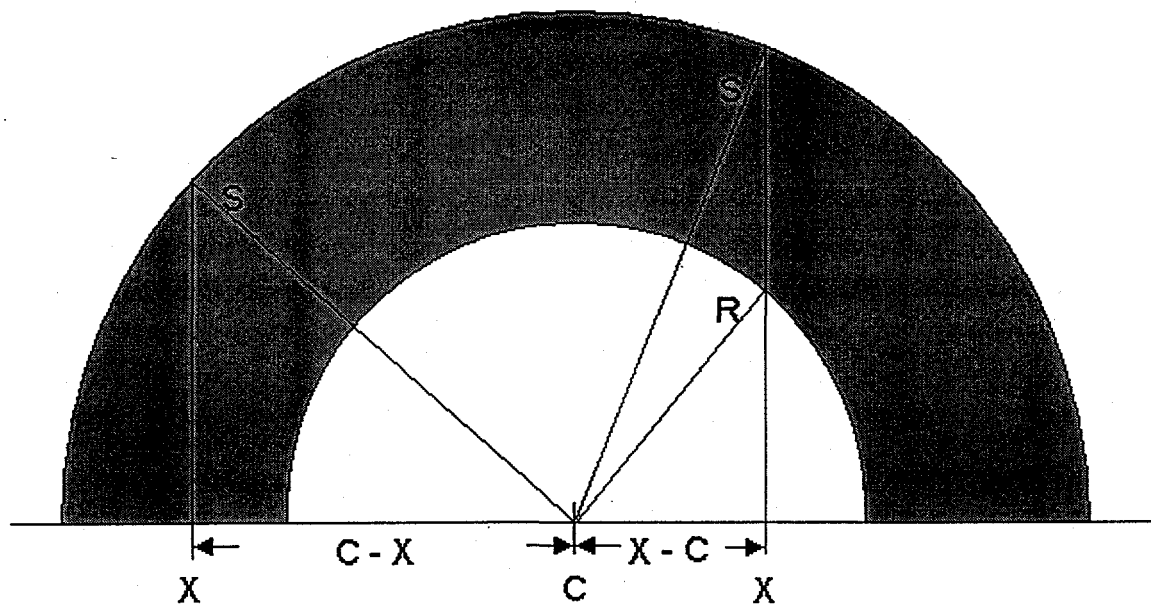


Figure 2. Schematic diagram for illustrating the origin of the formulas for relative transmissions.

SPECIAL FITTING PROCEDURES

Assuming that there is a reasonably good estimate of the center of this object, the plot can be divided into left and right halves. We then locate the smallest function value in each half. This gives an indication of the boundary between the inner cylinder and the core of the object. The average of these two positions will provide an estimate of the common center, C . Half the difference between these two positions will provide an estimate of the inner radius, R_2 , of the inner cylinder.

We then locate an interval of X values where we believe that $R_1 < X < S_1$. From this section of the graph, we can estimate the attenuation parameter b_1 and the outer radius S_1 of the outer cylinder. In the outer cylinder, let $Z = \log(Y)$, then

$$Z = 2b_1\sqrt{S_1^2 - (X - C)^2}. \quad (5)$$

Note that Z^2 is a linear function of $(X-C)^2$. This means that a straight line can be fit to the data and that the resulting coefficients can be used to estimate S_1 and b_1 .

We now use these parameter values to construct a hypothetical plot of the transmission through the outer cylinder. We locate where the actual graph deviates sharply from this newly constructed plot, and from this we locate an interval of X values where we believe that $R_2 < X < S_2$. Values from this section of the graph can be used to estimate the attenuation parameter b_2 and the outer radius of the inner cylinder S_2 . In this region, let $W = \log(Y)$, then

$$W - Z = 2(b_2 - b_1)\sqrt{S_2^2 - (X - C)^2} \quad (6)$$

since R_1 and S_2 are identical. Note that $(W-Z)^2$ is a linear function of $(X-C)^2$. This means that a straight line can be fit to the data and that the resulting coefficients can be used to estimate S_2 (which equals R_1) and the difference $b_2 - b_1$. From all of this, an estimate for b_2 is easy to generate. We now have initial estimates for all 7 of the parameters for the least squares algorithm.

DATA GENERATION

To test these procedures, we used computer algorithms to generate simulated data. We constructed a set of simulated data by first choosing the number of pixels that would represent the thickness of the inner cylinder. Then we created an ideal transmission plot using a default set of parameter values. To this we added various vectors of random, independent Gaussian noise whose standard deviations were either 1% or 3% of the transmission values. Each set consisted of anywhere from 25 to 100 different data plots. For each plot, we used the algorithm described above to produce initial estimates of the parameters. These estimates were then fed into a least squares algorithm for refinement. We stored the final parameter values so that we could calculate their means and standard deviations. We plotted the residuals of each fit to see if the least squares algorithm behaved abnormally.

We generated different sets of simulated data by varying the number of pixels to represent the inner cylinder and then setting the thickness of the outer cylinder to be ten times the thickness of the inner cylinder. We also varied the amount of noise added to the ideal transmission plot, but we did not blur the data prior to adding noise.

In each set of simulated data, the average of the values obtained for each parameter indicates whether the whole procedure suffers from any bias. The standard deviations of the values obtained for each parameter indicates the precision that can be expected from using this procedure.

The software we used to generate and analyze the simulated data consists of a collection of procedures and functions written in Interactive Data Language (IDL) from Research Systems Incorporated. The least squares algorithm is a modified version of the IDL routine called CURVEFIT[2]. CURVEFIT is an iterative nonlinear least squares procedure based on the Marquard-Levenberg algorithm [3].

RESULTS

In all of the sets of simulated data, the average of the parameter estimates indicates that there is no significant bias present in our procedure.

When we varied the number of pixels representing the inner cylinder from 1 to 10 and added 1% noise to the ideal plot, we achieved the optimal precision by using an inner cylinder thickness of only 5 pixels. We present the relative errors, in percent, that were achieved in the optimal case in Table 1. When we performed the same procedure with 3% noise, the relative errors were larger. Furthermore, our results were more ambiguous than in the case with 1% noise. Based on our simulation runs, we are uncertain what the optimal number of pixels for the thickness of the inner cylinder should be. The residual plots also indicated sporadic failures in the least squares algorithm. We present the relative errors, in percent that were achieved at a pixel scale of 10, in Table 2.

Table 1. Relative error of each parameter estimate in the case of 1% noise.

Parameter	Error in %
common center	.002
attenuation of outer cylinder	.2
outer radius of outer cylinder	.003
inner radius of outer cylinder	.03
attenuation of inner cylinder	6.
outer radius of inner cylinder	.04
inner radius of inner cylinder	.4

Table 2. Relative error of each parameter estimate in the case of 3% noise.

Parameter	Error in %
common center	.007
attenuation of outer cylinder	.8
outer radius of outer cylinder	.01
inner radius of outer cylinder	.4
attenuation of inner cylinder	16.
outer radius of inner cylinder	.5
inner radius of inner cylinder	.2

Figures 3, 4, 5, and 6 are plots of the relative errors for several parameters as a function of the width of the inner cylinder in pixels. Note in Figure 3 that in the worst case when the width of the inner cylinder is only one pixel, the relative error is less than .025%. This corresponds to an error in the radius measurement of .05 pixels. Also note in Figure 4 that in the worst case when the width of the inner cylinder is only one pixel, the relative error is about .3%. This corresponds to an error in the radius measurement of .6 pixels.

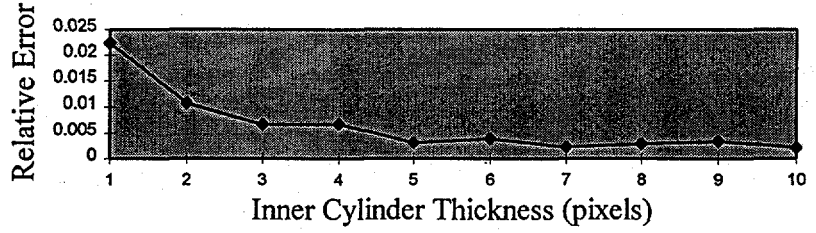


Figure 3. For 1% noise, the relative error (in percent) for the outer radius of the outer cylinder as a function of the thickness of the inner cylinder (in pixels).

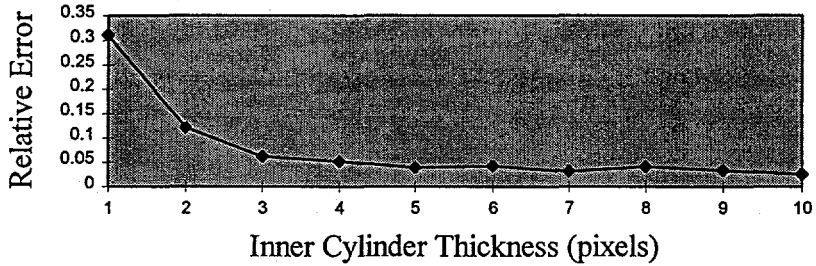


Figure 4. For 1% noise, the relative error (in percent) for the outer radius of the inner cylinder as a function of the thickness of the inner cylinder (in pixels).

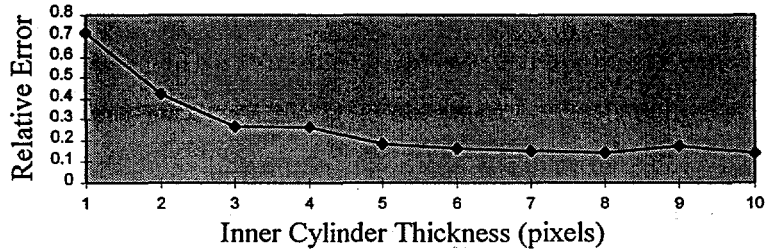


Figure 5. For 1% noise, the relative error (in percent) for the attenuation in the outer cylinder as a function of the thickness of the inner cylinder (in pixels).

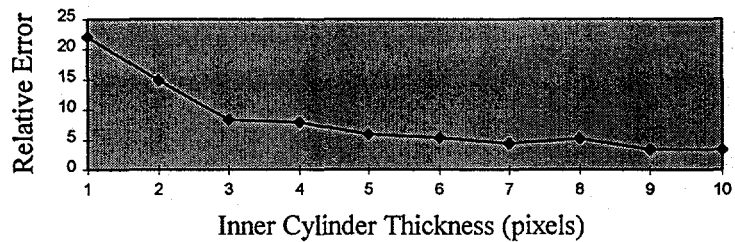


Figure 6. For 1% noise, the relative error (in percent) for the attenuation in the inner cylinder as a function of the thickness of the inner cylinder (in pixels).

SUMMARY AND FUTURE

Our results exhibit some promise that a least squares algorithm might be used in an automatic mode to examine objects that are axially symmetric and consist of two concentric cylinders. The results also emphasize the importance of keeping the rms noise in the image below 3%. Since the fitting process uses *a priori* knowledge about the objects being radiographed, other geometries would require different techniques for generating the initial parameter estimates.

In the future we plan to examine the effect of blurring on the performance of the least squares algorithm. The random independent noise that we now add to the data is not realistic. We intend to use a correlated noise function. A method for treating this kind of noise is given in [4]. We also plan to examine the maximum entropy algorithm which has received a lot of attention. A trimmed down version of Skilling and Bryan's [5] classic algorithm has been developed by Shaw and Tigg [6]. This algorithm has also been studied in conjunction with the tomographic reconstruction of radiographic images similar to the ones we have encountered. In support of this effort, we learned much from the work of Hanson [7,8].

REFERENCES

1. R.L. Whitman, H.M. Hanson, and K.A. Mueller, *Image Analysis for Dynamic Weapons Systems*, Los Alamos Report LALP-85-15, 1985.
2. *IDL Reference Guide*, Interactive Data Language Version 4, Research systems, Inc., 1995.
3. W. H. Press, B.P. Flannery, S.A. Teukolsky, and W.T. Vetterling, *Numerical Recipes in C*, Cambridge University Press, Cambridge, 1988.
4. K. M. Hanson, "Optimal object and edge localization in the presence of correlated noise," Proc. SPIE, 454 (1984) pp. 9-17.
5. J. Skilling and R.K. Bryan, "Maximum entropy image reconstruction: general algorithm," Mon. Not. R. Astr. Soc., 211 (1984), pp. 111-124.
6. W. T. Shaw and J. Tigg, *Applied Mathematics*, Addison-Wesley Publishing Company, New York, 1994.
7. K. M. Hanson, "A Bayesian approach to nonlinear inversion: Abel inversion from X-Ray attenuation data", in *Transport Theory, Invariant Imbedding, and Integral Equations*, eds. P. Nelson, V. Faber, T.A. Manteuffel, D.L. Seth, and A.B. White, Jr., Marcel Dekker, Inc., New York, 1989.
8. K. M. Hanson, "Introduction to Bayesian image analysis," Proc. SPIE, 1898 (1993) pp.716-731.